XXXVIII International School of Hydraulics, Lack, Poland

A presentation on

Discharge Characteristics of Triangular Weir with Upstream Ramp and its CFD Modelling using Ansys CFX Module

Presented by

SUBHOJIT KADIA, *M. Tech, Dept. of WRD & M*

BINIT KUMAR, *Research Scholar, Dept. of Civil Engg.*

ZULFEQUAR AHMAD, *Professor, Dept. of Civil Engg.*

Indian Institute of Technology Roorkee, *Uttarakhand-247667, India*

Date: 23rd May, 2019

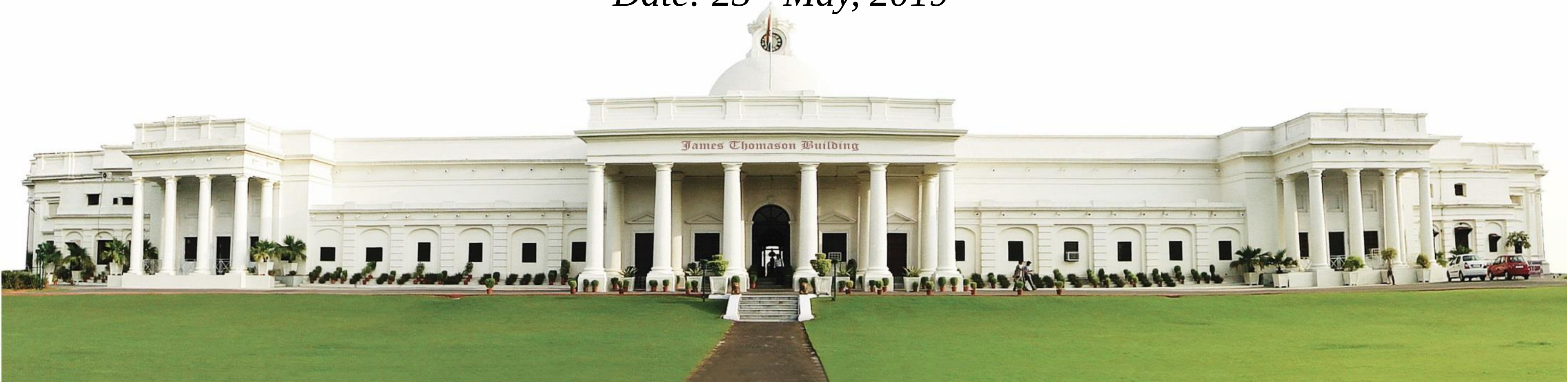

Contents

Introduction

- A transverse hydraulic structure like a weir affects the upstream flow condition and destabilises the sediment continuity (Bai and Duan 2014).
- The restriction in sediment passage results in deposition in the upstream of a weir and may scour in the downstream side (Kim et al. 2014).

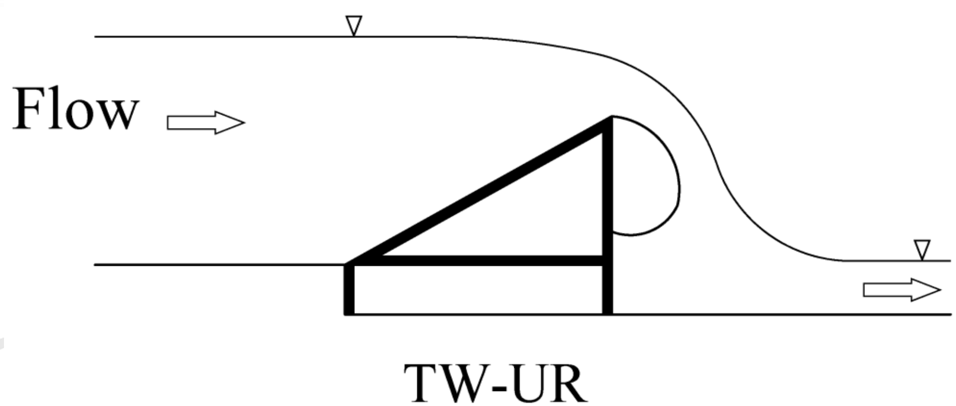

- A triangular weir with an upstream ramp (TW-UR) or a Piano Key Weir (PKW) has advantage of an adverse upstream bed than a sharp-crested weir (SCW) or broad crested weir (BCW).

Contd….

- According to Azimi and Rajaratnam (2009), weirs are divided into two groups: sharp-crested weirs (SCWs) and weirs of finite crest length.
- A TW-UR falls under the second group.
- The coefficient of discharge (C_d) for a TW-UR can be evaluated using the following basic equation used for a free flowing weir

$$Q = \frac{2}{3} C_d B \sqrt{2gH^3} \qquad (1)$$

Contd….

- Initially, Azimi et al. (2013) suggested Eq. (2), and later, Di Stefano et al. (2016) proposed Eq. (3) for the estimation of C_d.

$$C_d = 1.27\left(\frac{H}{L}\right)^{0.11} \Bigg/ \left(\sqrt{3}\left(\frac{P}{L}\right)^{1/10}\right) \tag{2}$$

$$C_d = 1.058\left(\frac{H}{P}\right)^{0.0839}\left(\frac{0.002}{P}\right)^{-0.0264}\left(1+\frac{L}{P}\right)^{0.1134} \Bigg/ \sqrt{3} \tag{3}$$

Contd….

- The coefficient of discharge for a SCW ($C_{d,sharp}$) is calculated using the Rehbock equation (Henderson 1966), Eq. (4).

$$C_{d,sharp} = 0.611 + 0.08\frac{H}{P} \qquad (4)$$

- The Computational Fluid Dynamics (CFD) simulation was used earlier for different weirs and it was found to be handy, accurate, time and cost saving tool.
- The present CFD simulation is on a TW-UR using Ansys CFX within Ansys 19.1 academic research version (ANSYS 2018).

Contd….

- Ansys CFX uses the finite volume and vertex-centered methods, whereas Fluent uses the finite volume and cell-centered methods (Acharya 2016; Berggren et al. 2009).
- The vertex-centered method is useful in reducing the computational space and cost due to a less number of degrees of freedom than the cell-centered method.

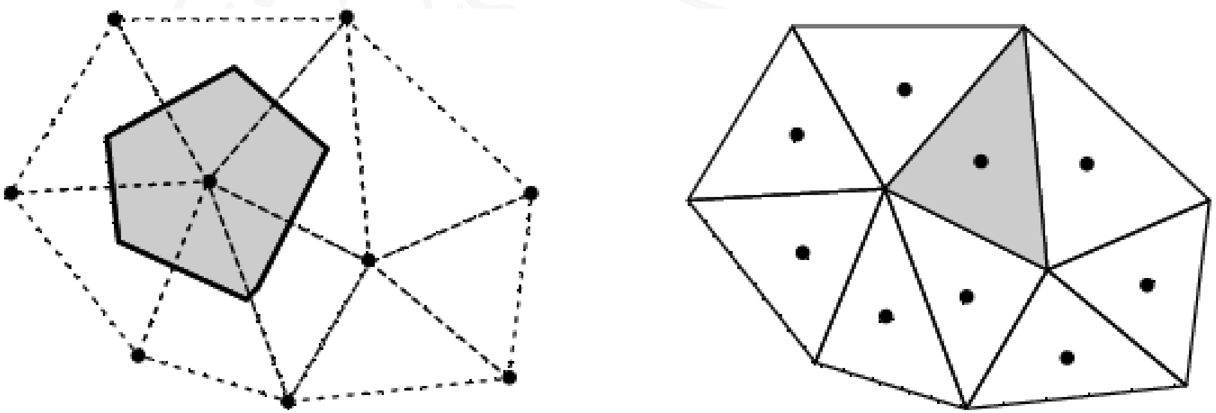

Vertex-centered vs cell-centered (Acharya 2016)

Objectives

1. **To study the head-discharge characteristics of a TW-UR through experimentation and CFD analysis.**
2. **Comparison between the flow fields obtained for TW-UR and SCW.**
3. **Checking the accuracy of the existing equations of the coefficient of discharge for TW-UR.**

Methodology

Experimental

Experimental

Model fabrication and setup preparation

Measurement of discharge and head over the weir crest

Input from experiments

CFD simulation

CFD simulation

Geometry design

Creation of **Meshing** after fixing size, method, solver, inflation, quality

Define **Model Physics**:
- Transient flow, time step and total time of simulation.
- Multiphase model and operating conditions setup.
- Setup of boundary conditions and domain initialisation.
- Define turbulent model (standard k-ε)
- Define transient scheme and convergence criteria.
- Define required outputs

Simulation run and comparison of results

Experimental setup

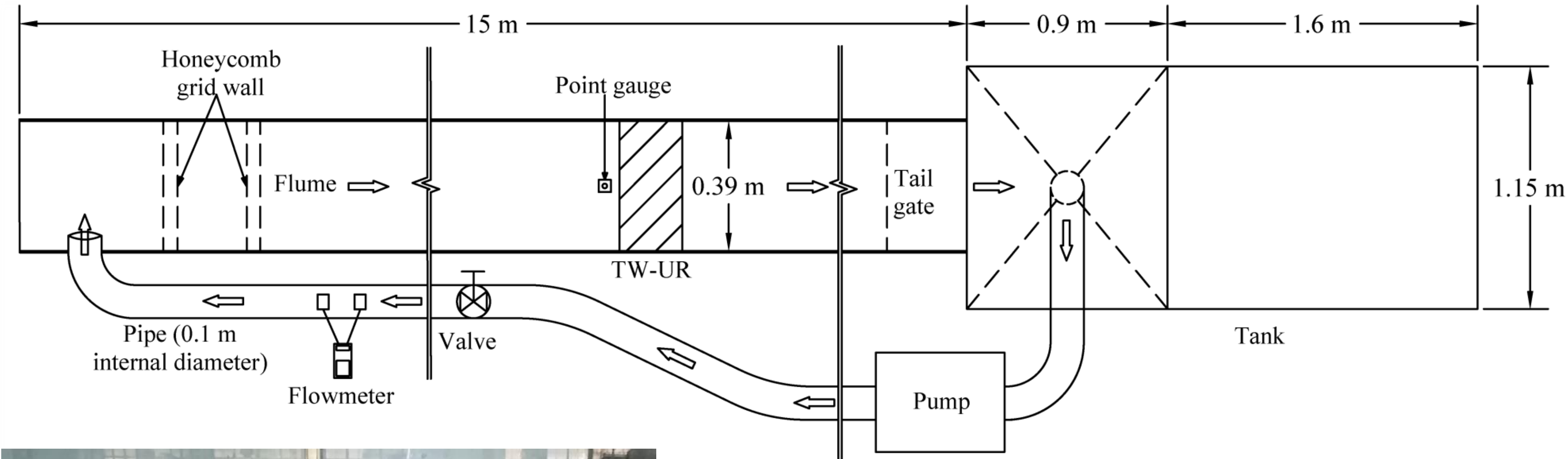

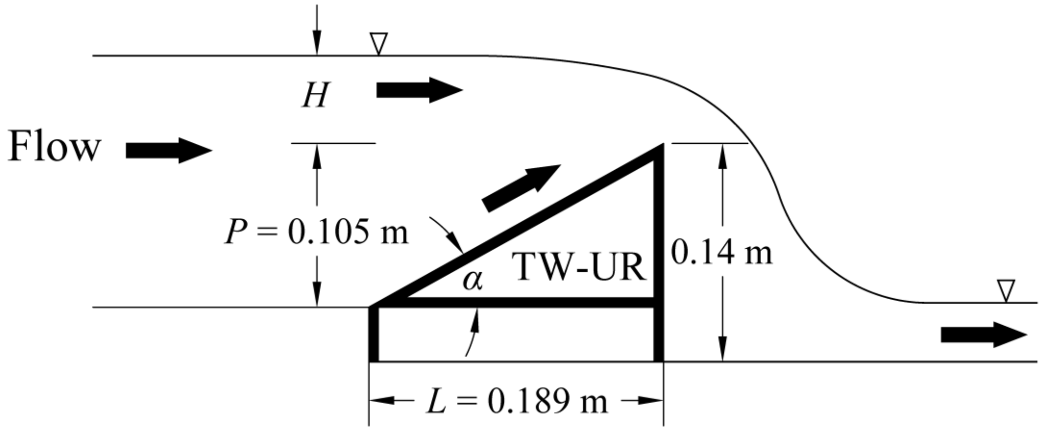

CFD simulation: boundary conditions

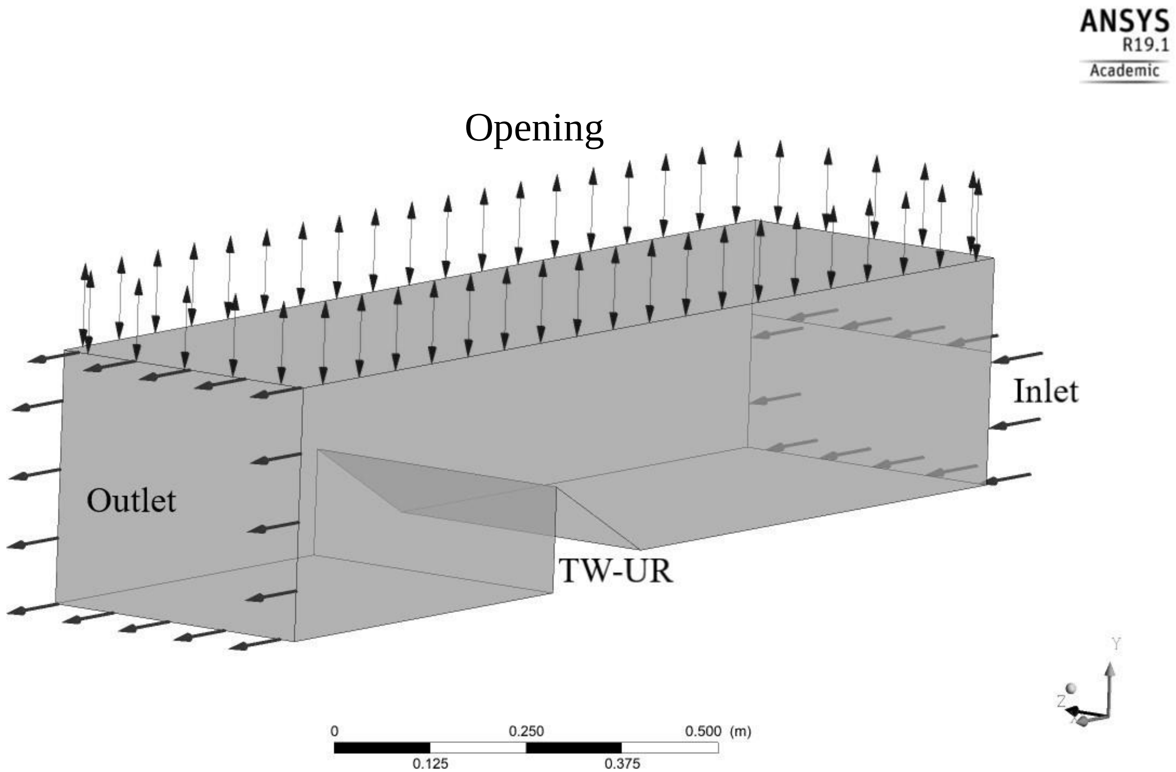

Boundary conditions

- **Inlet:** Mean velocity
- **Outlet:** Pressure based
- **Opening:** Relative pressure normal to the plane

Measurements and data collection

- Measurement of H at 0.2 m upstream of the weir crest for 23 discharges ranging from 7.3×10^{-3} m^3s^{-1} to 29.95×10^{-3} m^3s^{-1}.
- The simulation for TW-UR was performed for 5 discharges out of them. The free surface level was extracted by defining an Iso-clip having water volume fraction = 0.5.
- The velocity vector diagram at $Q = 20.96 \times 10^{-3}$ m^3s^{-1} was obtained along a longitudinal section for both TW-UR and SCW.

Contd….

- A total of 200 experimental datasets were collected to check the accuracy of the existing equations suggested by Azimi et al. (2013) and Di Stefano et al. (2016).

Table 1 Range of parameters for the present and previous investigations

Investigator	*L* [m]	*P* [m]	*H* [m]	Angle α
Abou-Seida and Quraishi (1976) (# group 2 case 1)	0.1415, 0.117, 0.0882,	0.0818, 0.117, 0.1527	0.0335 – 0.1273	30º, 45º, 60º
Bazin (# 125) (from Horton 1907)	0.167	0.50	0.30 – 0.427	71.6º
Shaker and Sarhan (2017)	0.06 – 0.30	0.06, 0.08, 0.10, 0.12	0.021 – 0.06	21.8º,26.6º, 33.7º, 45º
USDW (# 16) (from Horton 1907)	5.63	1.45	0.51 – 1.27	15.9º
Present study	0.189	0.105	0.0425 – 0.1055	29.1º

# indicates the number/set of the experiment.

Results and Discussion

Flow field obtained from CFD simulation

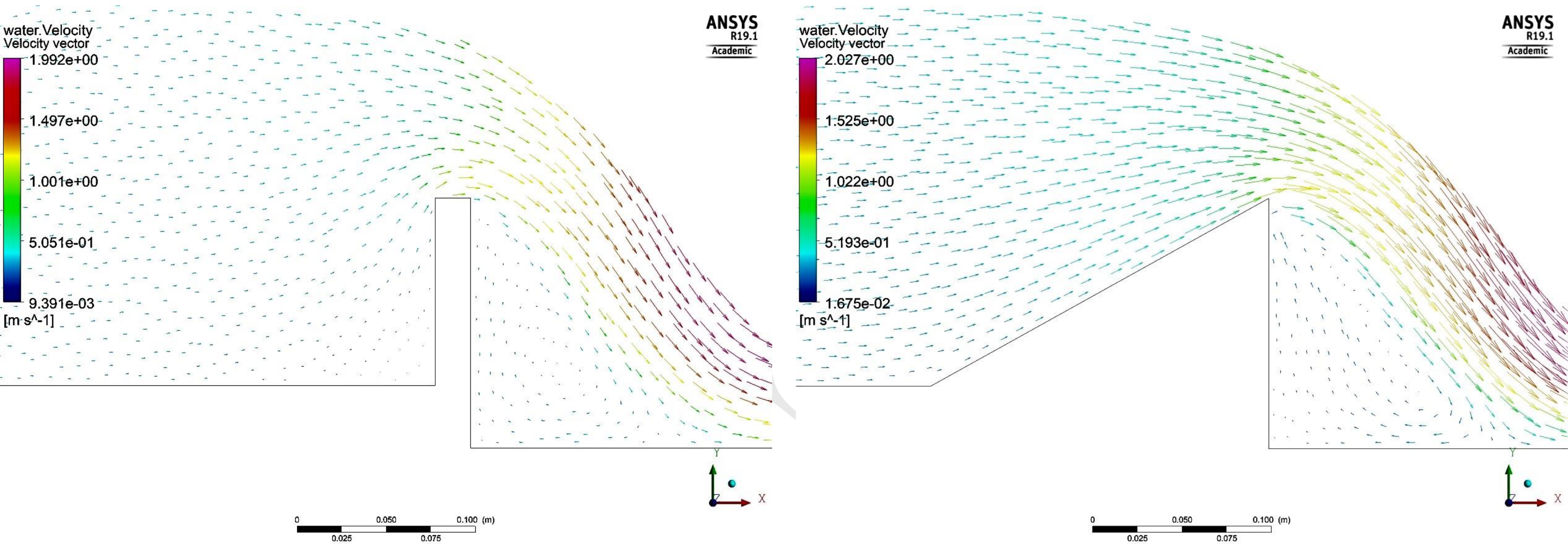

Flow field for a SCW and TW-UR at 20.76 × 10^{-3} m^3s^{-1} discharge

- TW-UR has more active flow field as compared to a SCW.
- Velocity increased along the flow due to flow contraction.
- Increases discharge capacity and possibility of sediment passage.

Air-water mixture and free surface

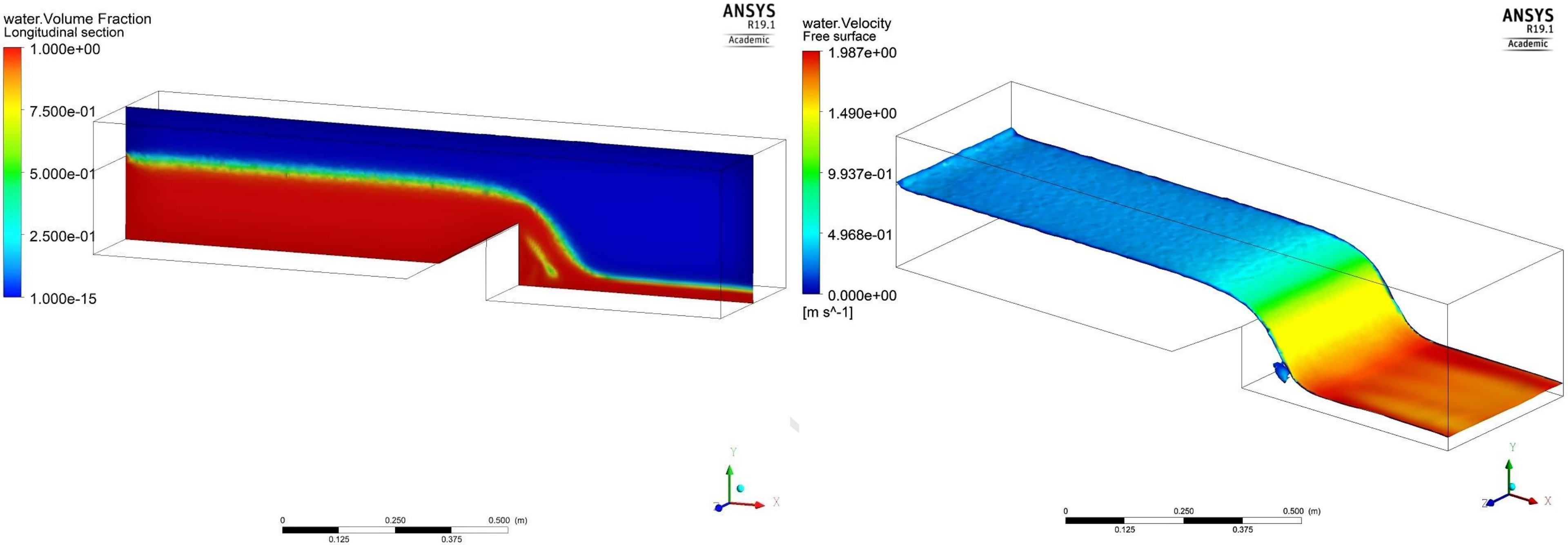

Simulated flow for TW-UR at 20.76 × 10^{-3} m^3 s^{-1} discharge:

air-water mixture and free surface

Simulated flow

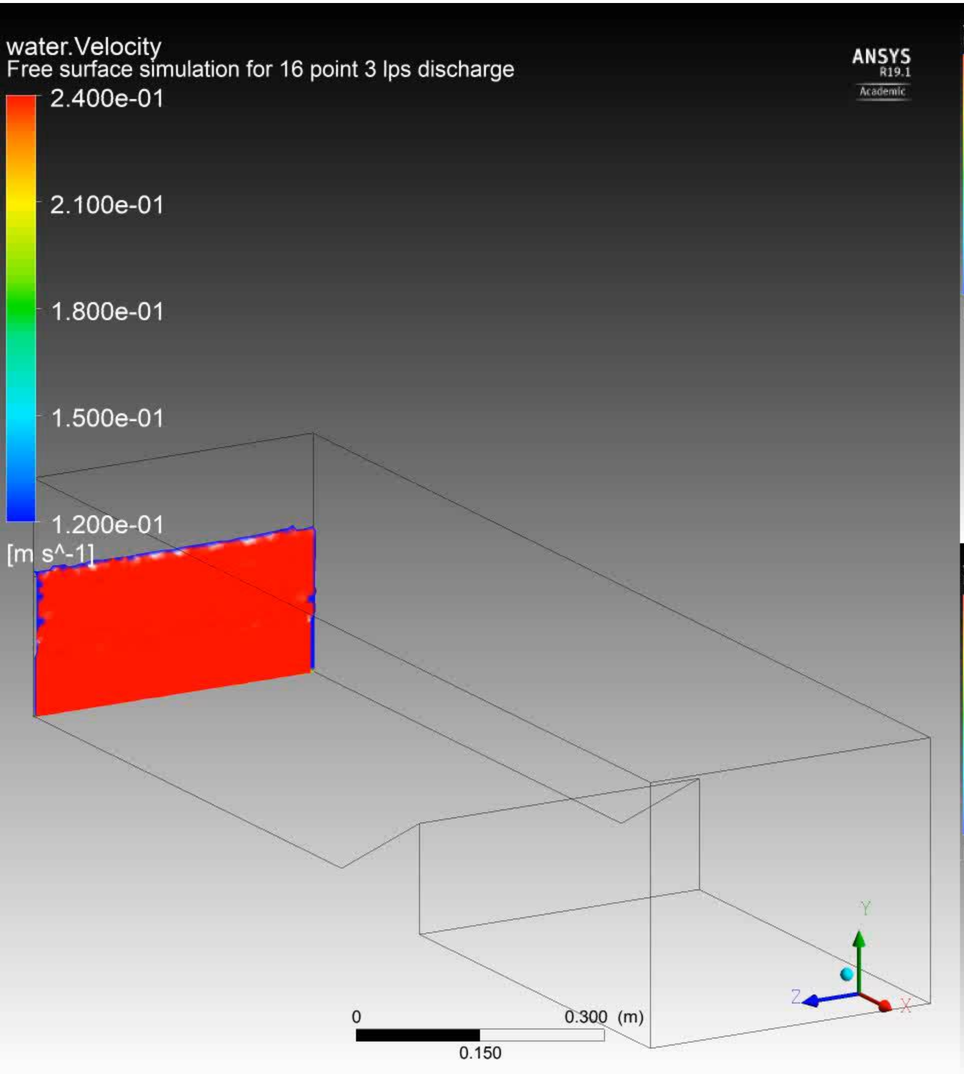

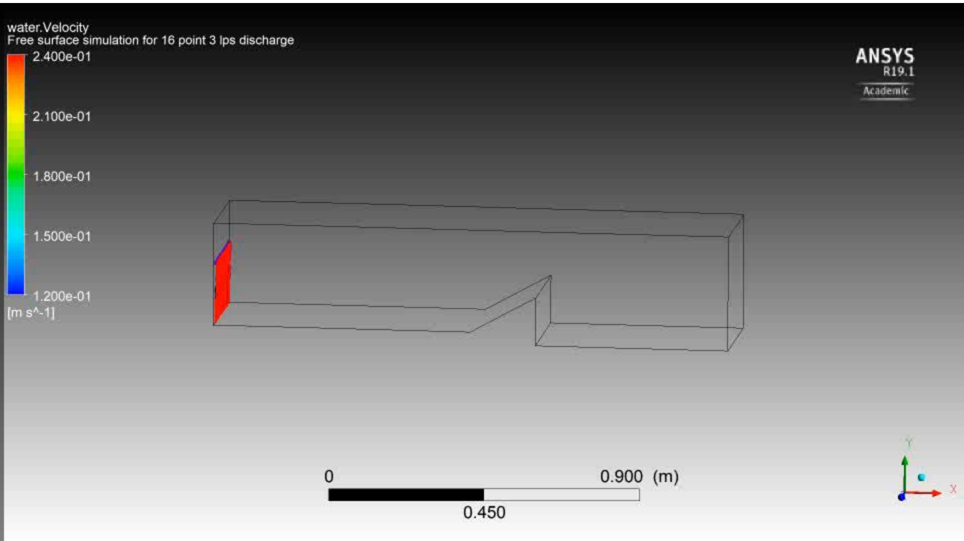

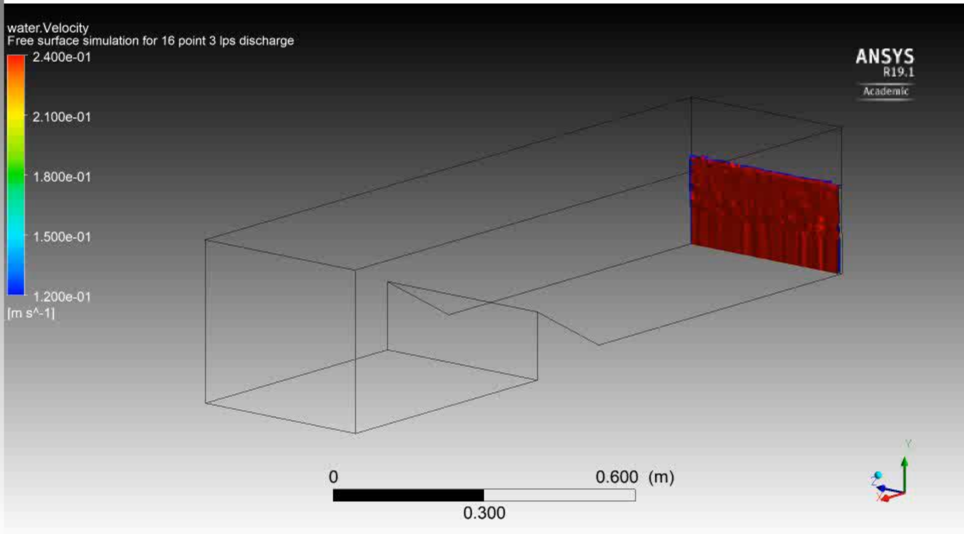

Comparison of the discharge obtained from CFD with the observed value

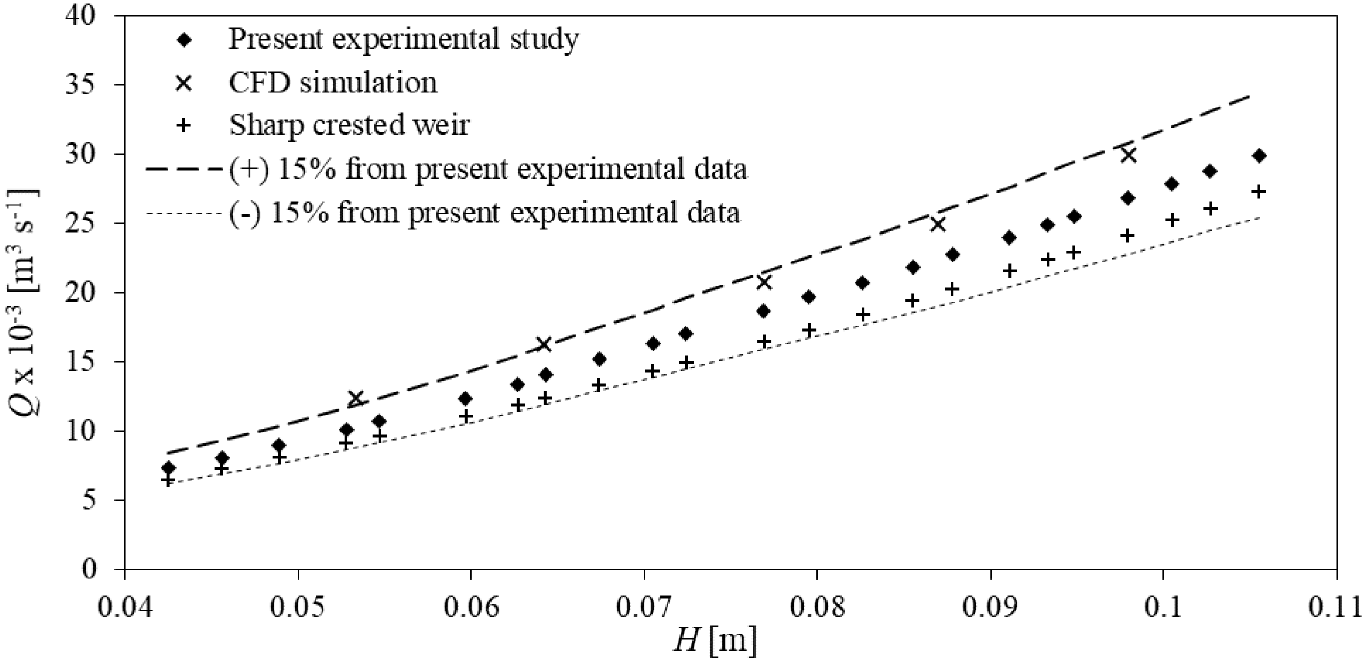

Head-discharge correlation

- TW-UR had about 9.8% to 14.3% higher discharging capacity than SCW.
- For TW-UR, CFD simulation estimated about 10% to 15% higher discharge under the same head in comparison to the observed results.
- C_d increased initially with H, but remained almost constant beyond $H/P \approx 0.65$

Checking the accuracy of existing equations for C_d

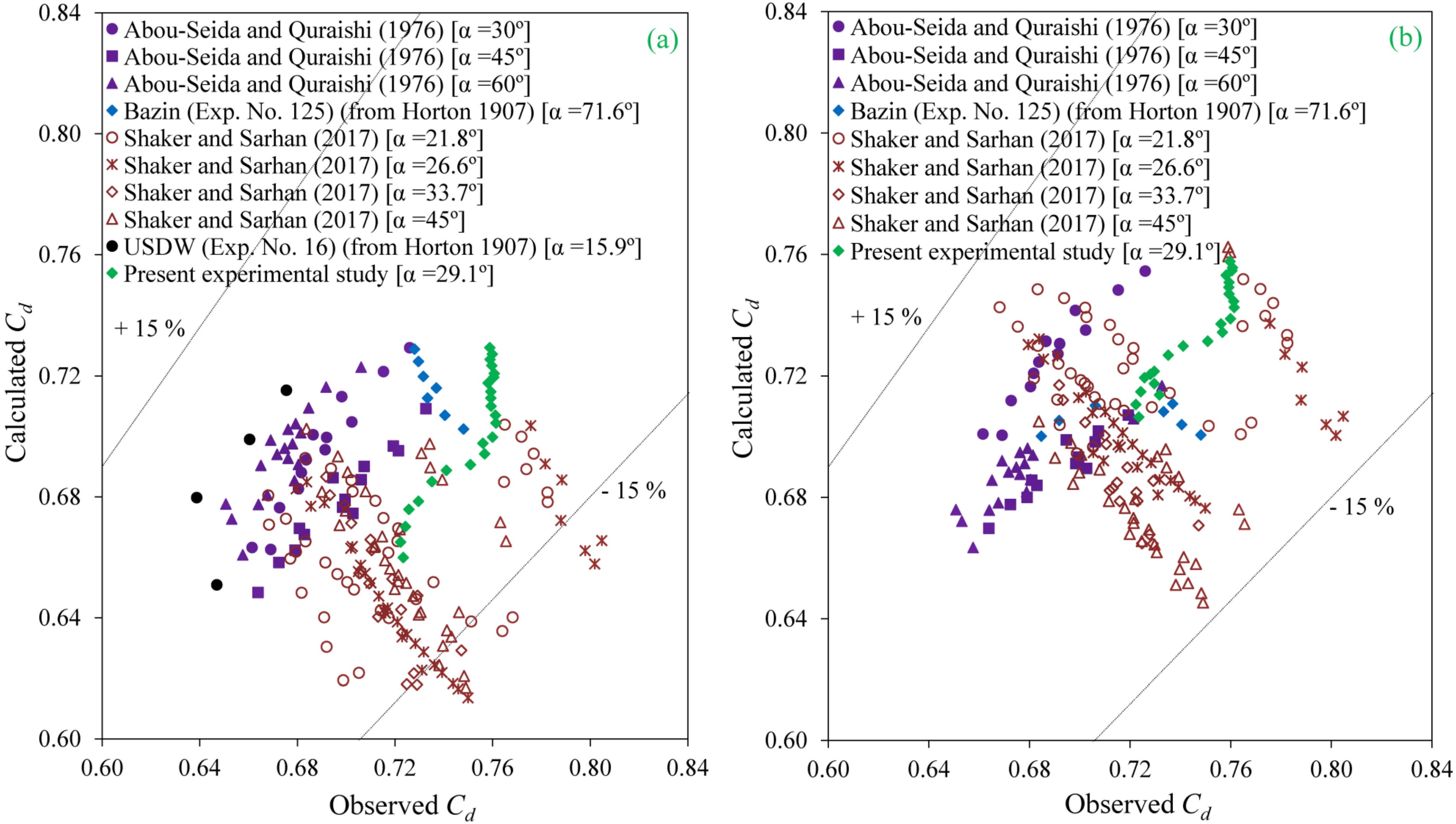

Calculated C_d vs observed C_d for: (a) Azimi et al. (2013), (b) Di Stefano et al. (2016)

Contd….

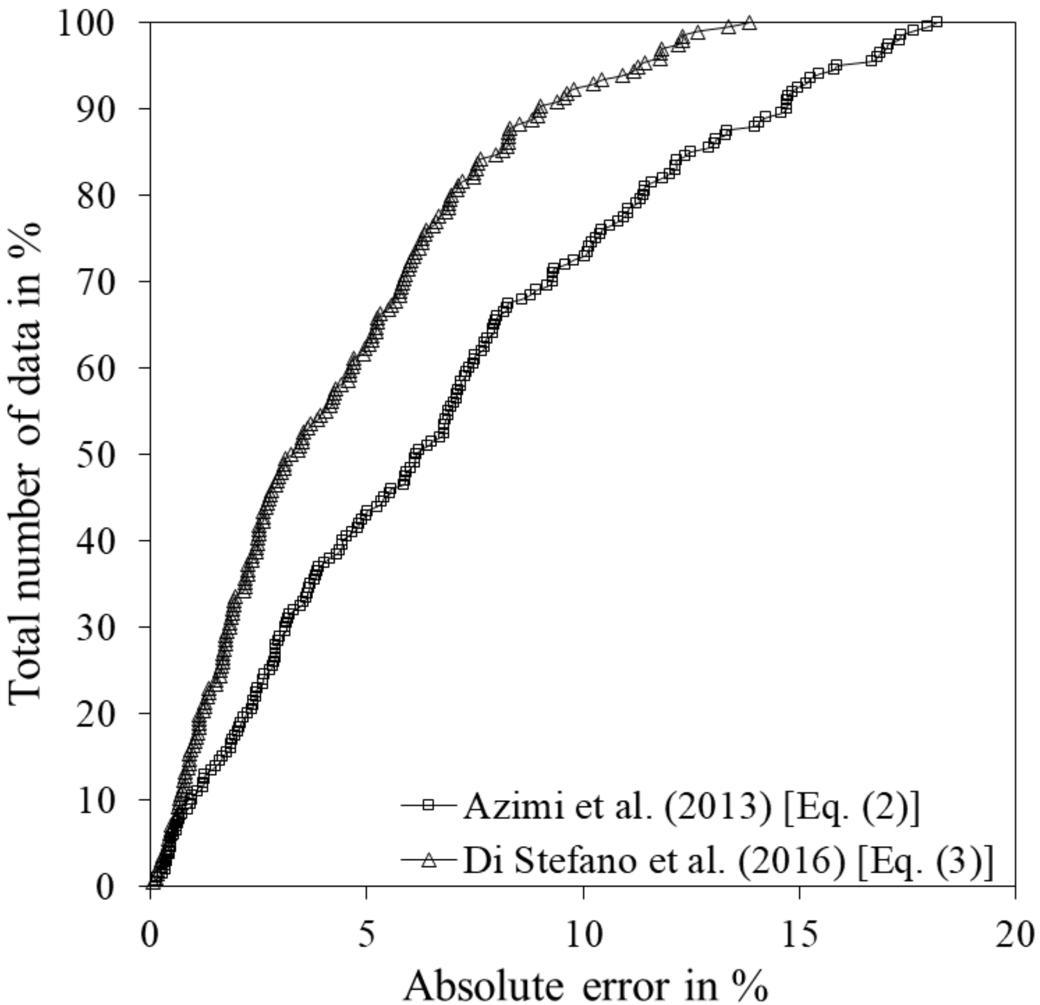

Total number of data vs absolute error

- The maximum absolute error for Eqs. (2)-(3) was 18.2% and 13.8%, respectively.
- The total number of datasets lay within 5%, 10% and 15% absolute error ranges for Eq. (2) was 43.0%, 72.5% and 92.5%, and for Eq. (3) it was 61.7%, 92.3% and 100%, respectively.

Contd….

- The equations were also evaluated based on two statistical parameters; mean absolute percentage error (*MAPE*) and root mean square error (*RMSE*) as suggested by Aydin and Emiroglu (2013); Aydin and Emiroglu (2016); Crookston et al. (2018):

$$MAPE = \frac{1}{N}\sum_{i=1}^{N}\left|\frac{C_{do} - C_{dc}}{C_{do}}\right| \times 100\%$$

$$RMSE = \sqrt{\frac{1}{N}\sum_{i=1}^{N}\left(C_{do} - C_{dc}\right)^{2}}$$

Contd….

Table 2 Error in C_d prediction for Eq. (2)-(3)

Investigator	Angle α	Eq. (2) (Azimi et al. 2013)		Eq. (3) (Di Stefano et al. 2016)	
		RMSE	MAPE (%)	RMSE	MAPE (%)
Abou-Seida and Quraishi (1976) (# group 2 case 1)	30°	0.008	0.91	0.037	5.40
	45°	0.019	2.67	0.009	1.07
	60°	0.020	2.84	0.015	2.05
Bazin (# 125) (from Horton 1907)	71.6°	0.025	2.67	0.028	3.37
Shaker and Sarhan (2017)	21.8°	0.066	7.59	0.039	4.57
	26.6°	0.091	10.86	0.050	5.58
	33.7°	0.073	8.98	0.039	4.55
	45°	0.074	8.84	0.059	6.92
USDW (# 16) (from Horton 1907)	15.9°	0.034	4.68	–	–
Present experimental study	29.1°	0.050	6.54	0.012	1.41
Total data	-	**0.062**	**6.86**	**0.04**	**4.30**

Conclusions

- A TW-UR model has higher discharging capacity than a SCW of same height (about 9.8% to 14.3% higher discharge was observed in the present study).
- The ramp and a highly active flow field in upstream of TW-UR are enhancing its discharging capacity and sediment passage capability than SCW and BCW.
- CFD simulation estimated about 10% to 15% higher discharge than observed value.
- Both graphical and statistical analysis has shown that the equation of C_d proposed by Di Stefano et al. (2016) is more accurate than the equation proposed by Azimi et al. (2013).

References

Abou-Seida MM, Quraishi AA (1976) A flow equation for submerged rectangular weirs. Proceedings of the Institution of Civil Engineers Part 2, 61:685–696

Acharya R (2016) Investigation of Differences in Ansys Solvers CFX and Fluent. Master Thesis, KTH Royal Institute of Technology, Stockholm, Sweden

ANSYS (2018) ANSYS Academic Research Mechanical and CFD, Release 19.1, Canonsburg, PA

Aydin MC, Emiroglu ME (2013) Determination of capacity of labyrinth side weir by CFD. Flow Measurement and Instrumentation 29:1–8

Aydin MC, Emiroglu ME (2016) Numerical analysis of subcritical flow over two-cycle trapezoidal labyrinth side weir. Flow Measurement and Instrumentation 48:20–28

Azimi AH, Rajaratnam N (2009) Discharge Characteristics of Weirs of Finite Crest Length. Journal of Hydraulic Engineering 135(12):1081–1085

Azimi AH, Rajaratnam N, Zhu DZ (2012) A note on sharp-crested weirs and weirs of finite crest length. Canadian Journal of Civil Engineering 39(11):1234–1237

Azimi AH, Rajaratnam N, Zhu DZ (2013) Discharge Characteristics of Weirs of Finite Crest Length with Upstream and Downstream Ramps. Journal of Irrigation and Drainage Engineering 139(1):75–83

Azimi H, Shabanlou S (2015) U-shaped channels along the side weir for subcritical and supercritical flow regimes. Flow Measurement and Instrumentation 46:170–178

Contd….

Bai Y, Duan JG (2014) Simulating unsteady flow and sediment transport in vegetated channel network. Journal of Hydrology 515:90–102

Bates PD, Lane SN, Ferguson RI (2005) Computational Fluid Dynamics: Applications in Environmental Hydraulics. John Wiley & Sons Ltd, Chichester

Berggren M, Ekström SE, Nordström J (2009) A discontinuous Galerkin extension of the vertex-centered edge-based finite volume method. Communications in Computational Physics 5(2-4):456–468

Bremer F, Oertel M (2017) Numerical investigation of wall thickness influence on Piano Key Weir discharge coefficients: A preliminary study. In: Proceedings of the Third International Workshop on Labyrinth and Piano Key Weirs 2017. Taylor & Francis Group, London, pp 101–108

Crookston BM, Anderson RM, Tullis BP (2018) Free-flow discharge estimation method for Piano Key weir geometries. Journal of Hydro-environment Research 19:160–167

Di Stefano C, Ferro V, Bijankhan M (2016) New theoretical solution of the outflow process for a weir with complex shape. Journal of Irrigation and Drainage Engineering 142(10):04016036-1–9

Fan J, Morris GL (1992) Reservoir Sedimentation. I: Delta and Density Current Deposits. Journal of Hydraulic Engineering 118(3):354–369

Garde RJ, Ranga Raju KG (2015) Mechanics of sediment transportation and alluvial stream problems. Revised third edition. New Age International (P) Ltd., New Delhi

Contd….

Henderson FM (1966) Open channel flow. Macmillan, New York

Horton RE (1907) Weir Experiments , Coefficients , and Formulas. Proc. U.S. Geological Survey- Water Supply and Irrigation (200), Government Printing office, Washington, DC

Hoseini SH, Jahromi SHM, Vahid MSR (2013) Determination of Discharge Coefficient of Rectangular Broad-Crested Side Weir in Trapezoidal Channel by CFD. International Journal of Hydraulic Engineering 2(4):64–70

Hu H, Qian Z, Yang W, Hou D, Du L (2018) Numerical study of characteristics and discharge capacity of piano key weirs. Flow Measurement and Instrumentation 62:27–32

Kim S, Im J, Lee SO (2014) Assessment of sediment exclusion efficiency for several modified labyrinth weirs. Paddy and Water Environment 12(Supp.1):133–140

Launder BE, Spalding DB (1972) Lectures in mathematical models of turbulence. Academic Press, London, New York

Launder BE, Spalding DB (1974) The Numerical Computation of Turbulent Flows. Computer Methods in Applied Mechanics and Engineering 3:269–289

Shaker AJ, Sarhan AS (2017) Performance of Flow over a Weir with Sloped Upstream Face. ZANCO Journal of Pure and Applied Sciences 29(3):43–54

Tiwari H, Sharma N (2017) Turbulence study in the vicinity of piano key weir: relevance, instrumentation, parameters and methods. Applied Water Science 7:525–534

THANK YOU